Module 4 : Third order nonlinear optical processes

Lecture 24 : Kerr lens modelocking: An application of self focusing

Objectives

This lecture deals with the application of self focusing phenomena to ultrafast laser technology. We will discuss

1. The basic principle to lock the phases of longitudinal modes oscillating in a laser cavity.
2. Active and Passive modelocking techniques.
3. Detailed design procedure for the Kerr lens mode locked Ti:Sapphire laser.

Laser modelocking techniques

Ultrashort laser pulses are required for probing ultrafast phenomena and multitude of other applications. We have shown in Lecture 6 that when the vast number of oscillating longitudinal modes in a laser cavity are superposed in a manner that their phases are locked together, superpose, an ultrashort wave packet in time emerges. This technique of ultrashort laser pulse generation is called modelocking. Here, we will discuss the application of nonlinear refraction and absorption for modelocking.

Let us now turn to the question of how mode-locking can be obtained qualitatively. To this end, we must invent mechanism by which the frequency ω and phase ϕ of a laser mode $E(\omega)$ can be coupled to the frequency ω_1 and phase ϕ_1 of the neighboring laser mode $E(\omega_1)$, the mechanism which can bridge the intermodal frequency gap ω'. Let us consider that the cavity losses are periodically modulated at frequency Ω. The field corresponding to frequency ω will then be given by

$$E(t) = E_0(1+\beta\cos\Omega t)\exp[-i(\omega t+\phi_0)]$$

$$= E_0\exp\left(-i\left(\omega t+\phi_0\right)\right)+\frac{\beta E_0}{2}\exp\left[-i\left(\omega+\Omega\right)t+\phi_0\right]+\frac{\beta E_0}{2}\exp[-i\left(\omega-\Omega\right)t+\phi_0] \qquad (24.1)$$

where β is the modulation depth, E_0 is the amplitude and ϕ_0 is the arbitrary constant phase. We can see from equation (24.1) that two new side bands emerge as a consequence of loss modulation. When the modulation frequency, $\Omega = \omega$, these side bands will coincide with the neighboring modes and will force them to oscillate in phase with $E(\omega)$. In a similar way $E(\omega_1)$will drive the next mode $E(\omega_2)$ etc. resulting in a chain of modes locked together in phase.

Cavity losses can be modulated in many different ways. Some of the examples are

1. **Active modelocking:** Cavity losses can be periodically modulated by placing an acoustoptic modulator driven by an external RF oscillator inside the laser resonator. The RF output of the oscillator is tuned to the inter-mode frequency interval.
2. **Synchronous modelocking:** When a mode-locked laser is employed to optically pump the gain medium of a laser whose cavity length and hence inter mode frequency separation are synchronized to the pump laser cavity, periodic gain modulation is produced. This results in mode-locking of the pumped laser.
3. **Passive modelocking:** Another way to produce mode-coupling is provided by a saturable absorber. In this case a saturable absorber is inserted between one of the cavity mirrors and the laser gain medium as shown in figure 24.1

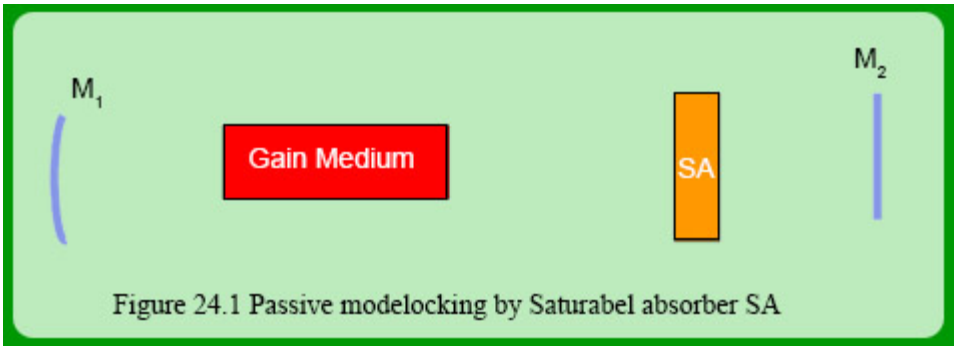

Figure 24.1 Passive modelocking by Saturabel absorber SA

When a fluctuation of the light intensity interacts with the saturable absorber, those parts of it whose

intensity is not high enough will be absorbed, but the other parts having sufficiently high intensity will be let through. In this way, the wings of the laser pulses are repeatedly cut away after every round trip and the light pulse becomes shorter and amplified through intensity dependent losses in the saturable absorber and gain in the cavity.

For the resonator of cavity of length*l*, loss modulation frequency $\varpi' = \pi c' / l$ (where *c*' is the effective speed of light in the resonator) equals the inter mode frequency gap. If we decompose the pulse into its individual stationary laser modes $\pm m\varpi'$, the interaction of these in the saturable absorber will lead to new side bands which automatically resonate with the neighboring modes and lead to efficient mode-locking. This is the passive mode-locking technique.

Passive mode-locking can also occur by the nonlinear polarization.

$$P\left(\varpi_{-1} = \left(\varpi - \varpi_1 + \varpi\right)\right) = \chi^{(3)}\left(-\varpi_{-1}; \varpi, -\varpi_1, \varpi\right) E\left(\varpi\right) E^{*}\left(\varpi_1\right) E(\varpi) \qquad (24.2)$$

due to the interaction of fields corresponding to mode frequency ω and its neighboring one at frequency $\varpi_1 = \varpi + \varpi'$. This polarization acts as driving force for the mode at frequency $\varpi_{-1} = \varpi - \varpi'$. In practical cases not only three modes (as in the example here) here interact but many (10^2-10^6). This leads to the possibility of self pulsing lasers where mode-locking results if the medium is pumped strongly.

To generate pulses much shorter than a picosecond, it is necessary to take into account of the group velocity dispersion (GVD) – the phenomenon which causes different frequency components to travel at different speeds, thereby broadening the pulses as they circulate in the laser cavity. The spectral width of the pulses is inversely proportional to their temporal duration and so as the pulses become shorter, they become more susceptible to GVD. The excessive GVD will prevent the generation of short pulses and so it should be minimized.

The net GVD experienced by pulses in the cavity can be reduced to minimum by introducing optical components such as prism pair which provide adjustable GVD of opposite sign to that arising from other intra cavity elements.

The first significant step in the ultrafast laser domain came in 1966 with the generation of pulses shorter than 10 ps by passive mode locking of Nd:glass laser. This achievement provided much of the stimulus for picosecond technology developments in the next decade. The passively mode-locked flash lamp pumped dye laser provided in 1968 both a decrease in pulse width (a few picosecond) and a wide extension of the wavelength range. Light pulses as short as 1.5 ps were generated in 1972 with the first operation of a cw dye laser. In 1981, with a bidirectional, colliding pulse mode locked ring dye laser, pulses of less than 100 fs were produced. Further manipulation of these pulses by self-phase modulation in a short optical fiber and compression with a grating pair led to the generation of pulses as short as 6 fs in 1987.

The experimental inconvenience of working with dyes and lack of broad tunable range led to the vibronic solid state media. In these systems, the strong coupling between vibrational energy states of host crystals and electronic energy states of the transition metal ions results in broad absorption and emission line widths. Ti^{3+}: Sapphire which exhibits an upper state life time of 3 μsec is a material with one of the highest gain cross section and provides the largest tunable range (680- 1130 nm) of any solid state laser media. Ti:Sapphire laser delivers output power of several watts unlike the few hundred milliwatts from dye lasers . Due to such a large gain line width which exceeds those of dyes by an order of magnitude, it emerged as potential medium for the ultrafast solid state laser.

The high intracavity powers in this laser have led to a new mode-locking technique, namely, the Kerr lens mode locking(KLM) which exploits the nonlinear intensity dependent refraction property of the gain medium itself. In the following we will describe in detail the design procedure which is based on theoretical model by Magni etal[1] and the calculations for the development of a self mode-locked (KLM) Ti:Sapphire laser in our laboratory. In this technique one exploits the change in the intracavity beam profile arising from self focusing due to the nonlinearity of the gain medium and translates it to intensity dependent losses like in the passive mode-locking by saturable absorber. This is achieved by appropriate aperturing of the beam in the cavity at a location where the beam diameter due to this nonlinear optical effect reduces and thus simulates/mimics the action of an ultrafast saturable absorber on account of reduced losses in the mode-locked (high power) operation than in cw (low peak power) operation(see figure 24.2).

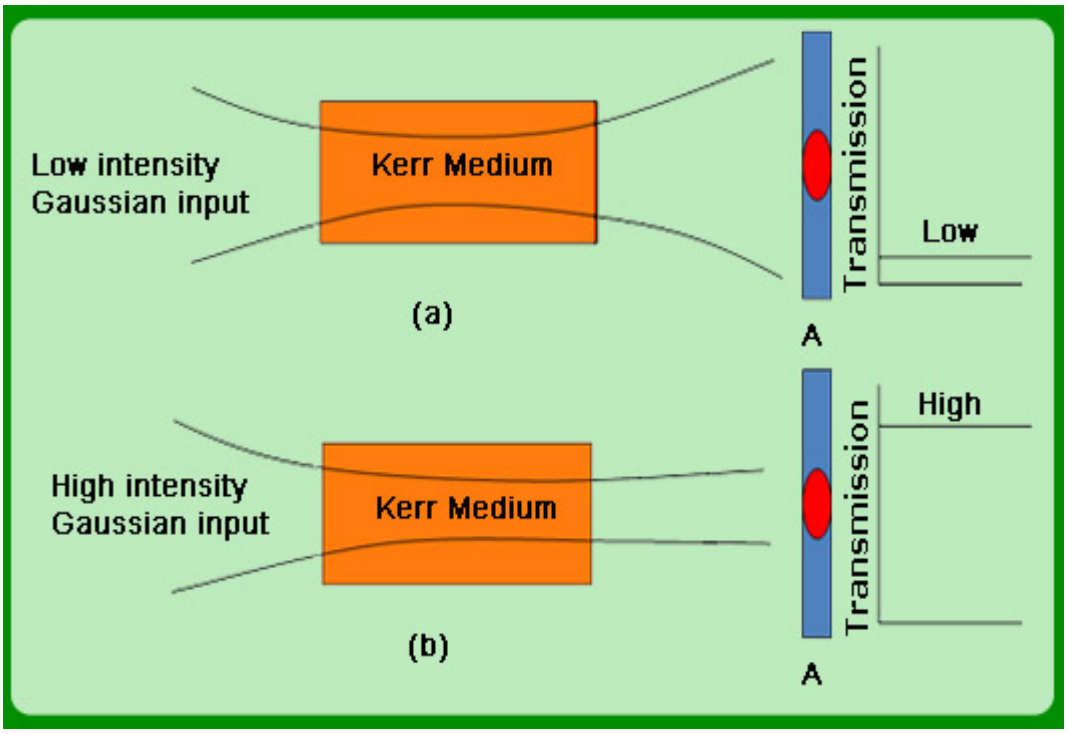

Figure 24.2 High transmission through the aperture A for (b) due to enhanced self focusing by nonlinear Kerr Medium

The key of Kerr lens mode-locking then lies in the cavity design enhancing the above effect.

Design of Self Mode-locked Ti:Sapphire laser

The resonator cavity used for the Ti:Sapphire laser is the astigmatically compensated Z-fold cavity shown in figure 24.3

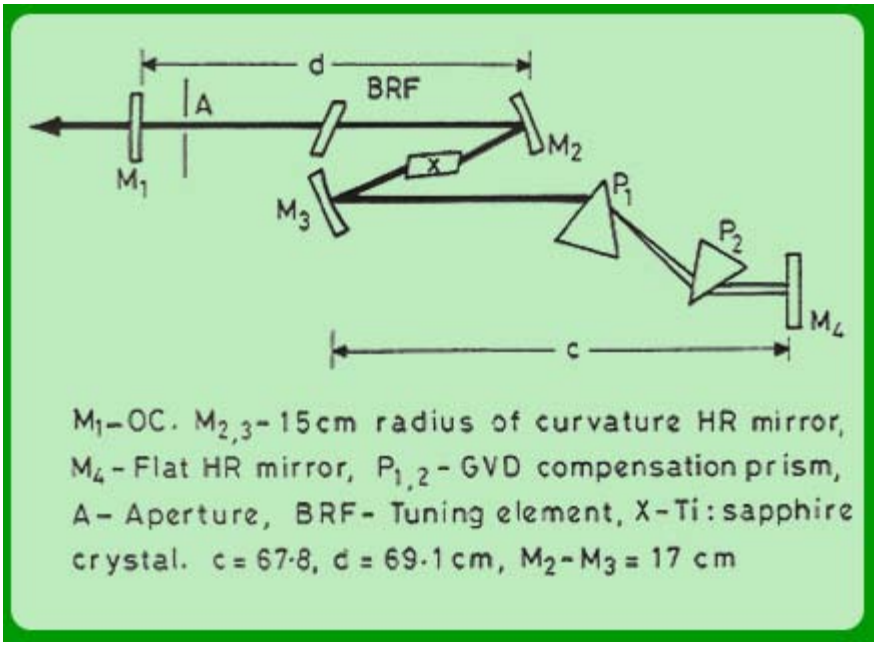

Figure 24.3 The z fold Resonator Cavity

It mainly consists of two plane mirrors M_1 and M_4 one of which is a high reflector (HR) and the other is an output coupler. Concave mirrors M_2 and M_3 behave like lenses for focusing the laser beam in to the gain medium i.e., the Ti:Sapphire crystal. The crystal has end faces cut at the Brewster's angle. It is so placed that the beam incident on it at Brewster's angle travels along the optical axis. This can be represented schematically as shown in figure 24.4.

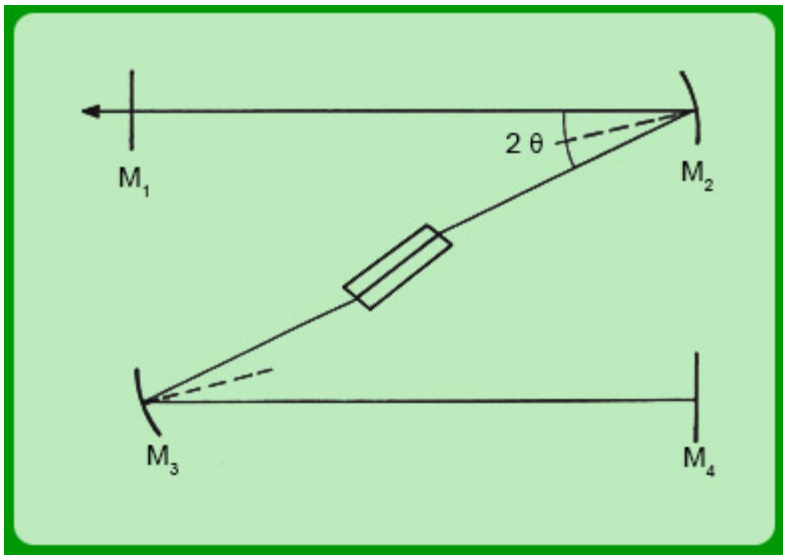

Figure 24.4 Schematic of the resonator cavity

The curved mirrors of radius of curvature R are astigmatic elements. They act as lenses of focal lengths fcosθ for the tangential beam and f/cosθ for the sagittal beam, where f=R/2 and θ is the angle of incidence on these mirrors. They are used to compensate the astigmatism introduced by the Brewster cut crystal faces. This compensation is achieved by a suitable choice of the radius of curvature of the mirrors and the fold angle θ. The gain medium itself acts like a convex lens due to the thermal gradient (caused by the pump and the modal beam profile) and the intensity dependent refractive index change (due to Kerr effect). Hence the equivalent cavity can be represented as in figure 24.5.

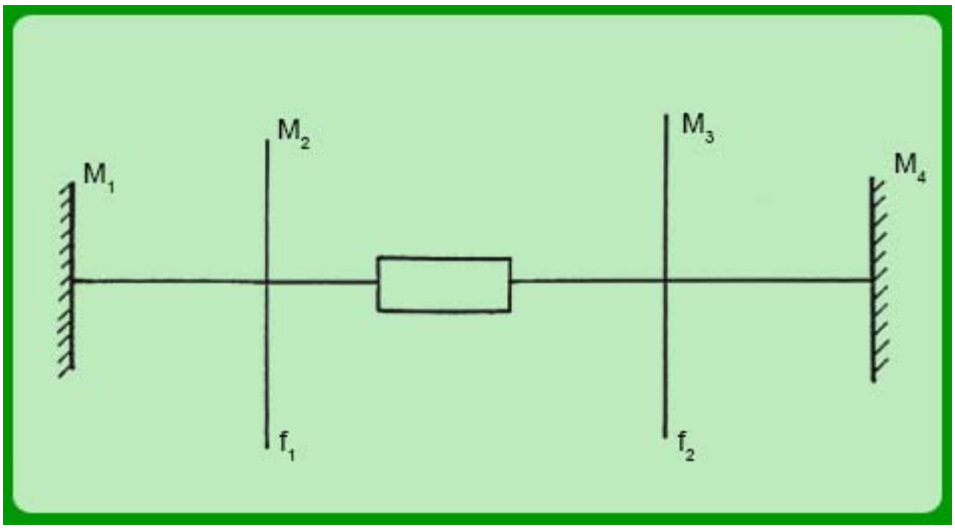

Figure 24.5 The equivalent of the z-fold cavity

In general, if the round trip ray matrix is given by

$$M = \begin{bmatrix} A & B \\ C & D \end{bmatrix} \tag{24.3}$$

At the end of the round trip the beam parameter q_1 gets modified to q_2.

$$q_2 = \frac{Aq_1 + B}{Cq_1 + D} \tag{24.4}$$

Where q's are the q-parameters of the Guassian beam. For a self consistent solution, $q_2 = q_1 = q$.

(24.5)

$$\frac{1}{q}=\frac{D-A}{2B}\pm\frac{1}{B}\left[\left(\frac{A+D}{2}\right)^2-1\right]^{0.5}$$

At the flat end mirror, q is real since the radius of curvature of the mirror is infinite. Therefore,

$$0\le\left(\frac{A+D}{2}\right)\le 1 \qquad (24.6)$$

The stability criteria for our linear resonator can be found by determining the solutions of the equivalent two mirrors resonator for which the standard solution exist. The radii of curvature of the equivalent resonator are

$$R_1=-\frac{f_1^2}{c-f_1} \qquad (24.7)$$

$$R_2=-\frac{f_2^2}{c-f_2} \qquad (24.8)$$

(see figures 24.3, 24.4 and 24.5 for the meanings of various terms in these equations) and $t = R_1+R_2+\delta$ where δ = (a + b) - (f_1 + f_2). If we assume that $|R_2|$ $|R_1|$, d_1 $f_1$and d_1 f_2, stable operation for this configuration is possible for two separate ranges,

$$0<\delta<-R_2 \qquad (24.9)$$

$$-R_1<\delta<-R_1-R_2 \qquad (24.10)$$

For our resonator cavity, these equations translate to

$$0<\delta<\frac{f^2}{d-f} \qquad (24.11)$$

and

$$\frac{f^2}{c-f}<\delta<\frac{f^2}{d-f}+\frac{f^2}{c-f} \qquad (24.12)$$

Figure 24.6 gives a schematic of the regions of stability.

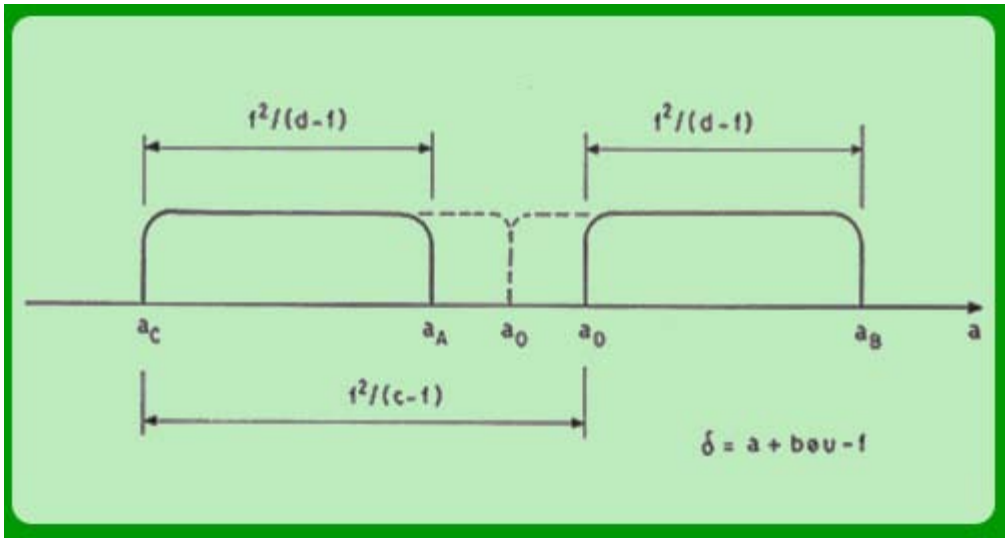

Figure 24.6 The range of δ for which the laser operates in a stable region

The beam radius at the output coupler of the short arm is notably larger for the range 0 δ $-R_2$ than for $-R_1$ δ $-R_1-R_2$, whereas the radius at the output coupler of the long arm is comparable for both

stability ranges.

Optimization of cavity for Kerr Lens Mode-locking:

Consider the nonlinear integral transmission of the aperture T (Γ) where Γ (ω_4)= ω_s/ω_4 is the normalized aperture radius and ω_s is the aperture radius. If $S(x,y)$ is the aperture intensity transmission function then

$$T(\Gamma)=\int_{-\infty}^{\infty}\int_{-\infty}^{\infty}dxdyS(x,y)\frac{2}{\pi\omega_4^2}exp\left[\frac{-2\left(x^2+y^2\right)}{\omega_4^2}\right] \tag{24.13}$$

Due to the self-focusing effect the spot size changes from its zero power value ω_4^0 to ω_4 = ω_4^0 + $\Delta\ \omega_4$.

Using Taylor series expansion for T about the zero power value $\Gamma_0=\omega_s/\omega_4$, we get

$$T(\Gamma)=T(\Gamma_0)-(\Gamma_0)\frac{\partial T}{\partial\Gamma}\frac{\Delta\omega_4}{\omega_4^0}=1-q_l-q_{nl}\frac{\Delta\omega_4}{\omega_4^0} \tag{24.14}$$

where q_l and q_{nl} denote the linear and nonlinear loss coefficients.

In order to achieve maximum differential between the cw and the mode locked operations, the cavity configuration has to be optimized. To calculate the optimum cavity parameters we have to maximize the nonlinear loss (as in case of passive mode locking with a saturable absorber) i.e., we have to optimize the function

$$F=-\frac{1}{\omega_4^0}\left(\frac{\partial\omega_4}{\partial p}\right)_{p\to lowpower} \tag{24.15}$$

$$=1-\left(\frac{\omega_4}{\omega_4^0}\right)_{p\to lowpower} \tag{24.16}$$

where ω_4 - spot size at the aperture with nonzero cavity power, ω_4^0 - spot size at the aperture with zero cavity power and p - power lasing in the laser cavity. This function is essentially a measure of the sensitivity of the cavity to the intensity dependent variation in the spot size on the intracavity aperture and hence its nonlinear transmission.

Interaction of the nonlinear medium with the radiation field modifies its refractive index. This change in refractive index is power dependent. The change of refractive index of the medium is due to the power oscillating in the cavity and the increase in temperature of the gain medium

$$n(x,y)=n_0+\frac{\partial n}{\partial\theta}\Delta\theta(x,y)+n_2I(x,y) \tag{24.17}$$

Where n_0 is the linear refractive index, n_2 is the nonlinear refractive index, $\theta(x, y)$ is the radially varying temperature, $I(x, y)$ is the beam intensity in the medium. Usually the change Δn due to the thermal effects is unimportant for self mode-locking in comparison with the intensity dependent term. Therefore,

$$n=n_0+2n_2|u|^2 \tag{24.18}$$

The paraxial wave equation

$$\frac{\partial^2u}{\partial x^2}+\frac{\partial^2u}{\partial y^2}-2jk\frac{\partial u}{\partial z}=0 \tag{24.19}$$

Equation 24.19 can be written as[1]

$$\nabla_T u-2jk\frac{\partial u}{\partial z}+k^2\frac{n_2}{n_0}|u|^2u=0 \tag{24.20}$$

Where ∇_T is the transverse Laplacian operator, $k=n_0\omega c$ is the wave vector and c is the velocity of light

in free space. The above equation has a Gaussian spherical function as the fundamental solution for moderate nonlinearity. We therefore look for solutions of the form

$$u(r,z)=\frac{U}{\omega(z)}exp\left[-\left(\frac{r}{\omega(z)}\right)^2-\frac{jkr^2}{2R(z)}+j\phi\right] \tag{24.21}$$

where $r^2=x^2+y^2$ is the radial distance from the z-axis, U is the real field amplitude.

We can approximate the intensity profile as a parabola

$$|u|^2=\frac{U^2}{\omega^2}\left(1-\frac{ar^2}{\omega^2}\right) \tag{24.22}$$

In the above equation, the factor *a* accounts for the correction due to the neglect of higher order terms in the expansion. Numerically as well as experimentally it has been found that *a* lies between 3.77 and 6.4. Using the above expression we get the solution of equation (24.20) as

$$\omega(z)^2=\omega_1^2\left[\left(1+\frac{z}{R_1}\right)^2+\left(\frac{\lambda z}{\pi n_0\omega_1^2}\right)^2\left(1-\frac{P}{P_c}\right)\right] \tag{24.23}$$

$$\frac{1}{R(z)}=\left(\frac{\omega_1}{\omega(z)^2}\right)\left[\frac{1}{R_1}+\frac{z}{R_1^2}+z\left(\frac{\lambda}{\pi n_0\omega_1^2}\right)^2\left(1-\frac{P}{P_c}\right)\right] \tag{24.24}$$

$$\phi(z)-\phi_1=\frac{1-\frac{3P}{P_c}}{\sqrt{1-\frac{P}{P_c}}}\left[arctan\left(\frac{\pi n_0\omega^2(z)}{\lambda R(z)\sqrt{1-\frac{P}{P_c}}}\right)-arctan\left(\frac{\pi n_0\omega_1^2(z)}{\lambda R_1\sqrt{1-\frac{P}{P_c}}}\right)\right] \tag{24.25}$$

where R_1 and ω_1 are the initial values of the radius of curvature and spot-size.

$$P_c=\frac{a\lambda^2}{8\pi n_2 n_0} \tag{24.26}$$

is called the critical power. For a Ti:Sapphire laser, typically P_c=2.6 MW.

The above equations completely characterize beam propagation through the nonlinear medium. As can be seen from the equation, the only modification in the beam on propagating through the nonlinear medium is that its confocal parameter is modified by a factor η where

$$\eta=\frac{1}{\sqrt{1-\frac{P}{P_c}}} \tag{24.27}$$

The ray matrix for the Kerr medium can be written as

$$M=\sqrt{1-\gamma}\begin{bmatrix}1 & \frac{d}{n_0}\\ -\frac{\gamma n_0}{1-\gamma} & 1\end{bmatrix} \tag{24.28}$$

where

$$\gamma=\frac{P}{P_c}\left[1+\left(\frac{\pi n_0\omega_1^2}{d\lambda_0}\right)^2\left(1+\frac{d}{R_1}\right)^2\right]^{-1} \tag{24.29}$$

The above equation is valid only for the case of a cylindrically symmetric Gaussian beam. If the tangential and the sagittal plane beams incident on the crystal at Brewster's angles are considered independently, then the B element of the matrix is d/n_0^3 for the tangential beam and d/n_0 for the sagittal beam.

For the more general case of an elliptical beam, we have to take in to account the coupling of the sagittal and tangential plane beams. For the coupled case the above matrix is modified as,

$$M_i = \sqrt{1-\gamma_i}\begin{bmatrix} 1 & \frac{d}{n_0} \\ -\frac{\gamma_i n_0}{1-\gamma_i} & 1 \end{bmatrix} \tag{24.30}$$

where $i = x,y$, $\gamma_x = r(z)\gamma$ and $\gamma_y = \gamma/r(z)$where $r(z) = \omega_x(z)/\omega_y(z)$.

The propagation of the beam through the nonlinear cavity can then be described by the ABCD matrix method. The round trip matrix through the cavity shown in figure 24.5 is

$$M = \begin{bmatrix} A & B \\ C & D \end{bmatrix}$$

$$= \begin{bmatrix} a_2 & b_2 \\ c_2 & d_2 \end{bmatrix}[K.M]\begin{bmatrix} d_1 & b_1 \\ c_1 & a_1 \end{bmatrix} \tag{24.31}$$

where the central matrix gives the ray transformation introduced by the Kerr medium, i.e., the crystal.

$$\begin{aligned} a_1 &= 1-d/f & a_2 &= 1-c/f \\ b_1 &= b+d-bd/f & b_2 &= a+c-ac/f \\ c_1 &= -1/f & c_2 &= -1/f \\ d_1 &= 1-b/f & d_2 &= 1-a/f \end{aligned} \tag{24.32}$$

We can calculate the spot size of the cavity beam on output coupler using equation 24.4 as a function of intra cavity power and the function F defined by equation 24.16 can be evaluated. One then optimizes cavity configuration maximizing this function and hence favoring mode-locking.

We choose to operate the laser in the stability region given by eqn. (24.10). At the edge of the stability border we have

$$a = a_d = 2f - b + \frac{f^2}{c-f} \tag{24.33}$$

For stable operation, we increment a by a small amount so as to work away from the stability border by a_{0u}, therefore

$$a = a_d + a_{0u} \tag{24.34}$$

To maximize F, the cavity parameters are so chosen that the two stability borders lie close to each other. So let $d_0 = c$. Let $d = d_0 + d_{0u}$ and $b = b_{ou} + f$, where b_{0u} is the distance between the center of the crystal and the local plane of M_3. With $\delta = a + b - 2f$, we get

$$\delta = \frac{f^2}{c-f} + a_{0u} \tag{24.35}$$

i.e., we are always in the stability region given by equation 24.12. The factor b_{0u} was varied about the mean value of f and the corresponding F value was plotted against b_{0u}. The graph shown in figure 24.7 shows the F function maximized for the output coupler placed at the end mirror of the long arm of the resonator. The graph in figure 24.8 shows the F function maximized for the output coupler placed at the end mirror of the shorter arm of the resonator.

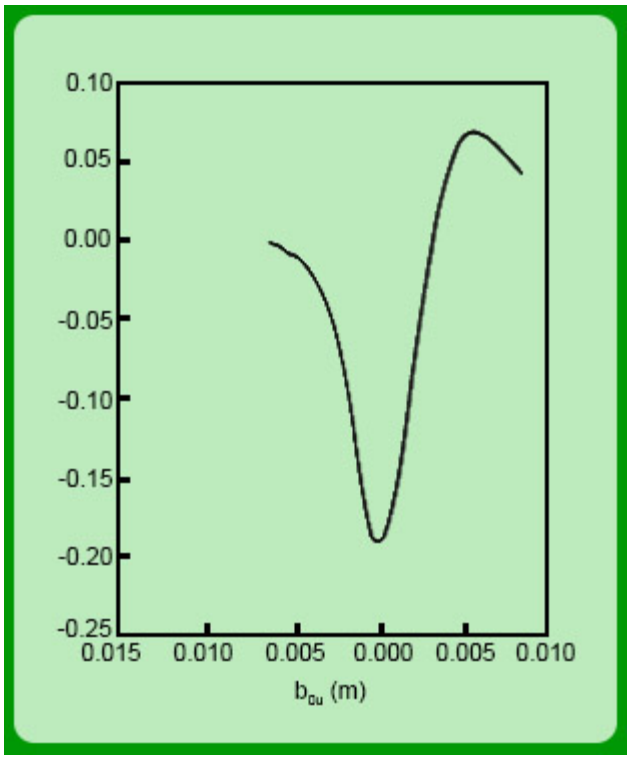

Figure 24.7 F-parameter optimized for OC in long arm

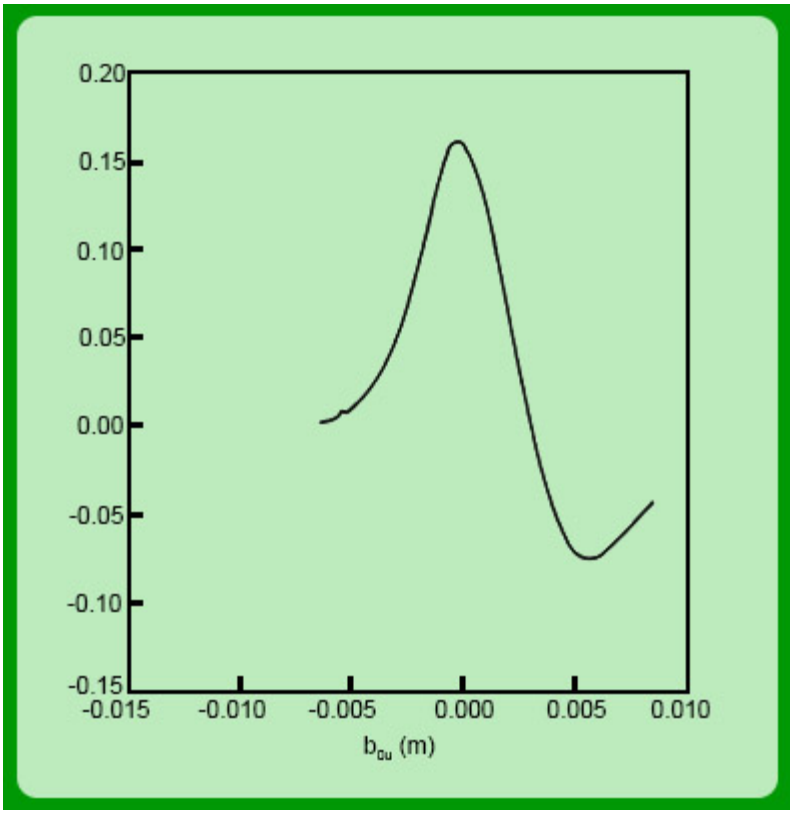

Figure 24.8 F-parameter optimized for OC in short arm

As can be seen from the two graphs, the *F* function is more sensitive to the crystal placement for the OC in the shorter arm, however, it is more stable around the peak region for the OC at the longer arm end.

It is seen that the *F* function is highly sensitive to the distance away from the stability border at which we operate. Figure 24.9 shows the dependence of the *F* function on the a_{0u} parameter. The closer we are to the stability border, the more peaked is the *F* function.

Hence it is found that *F* is maximized for

- a symmetrical cavity i.e. d = c.
- when operation is close to the stability border.
- cavity parameters must be chosen such that the borders of the two stability regions must lie close to each other.

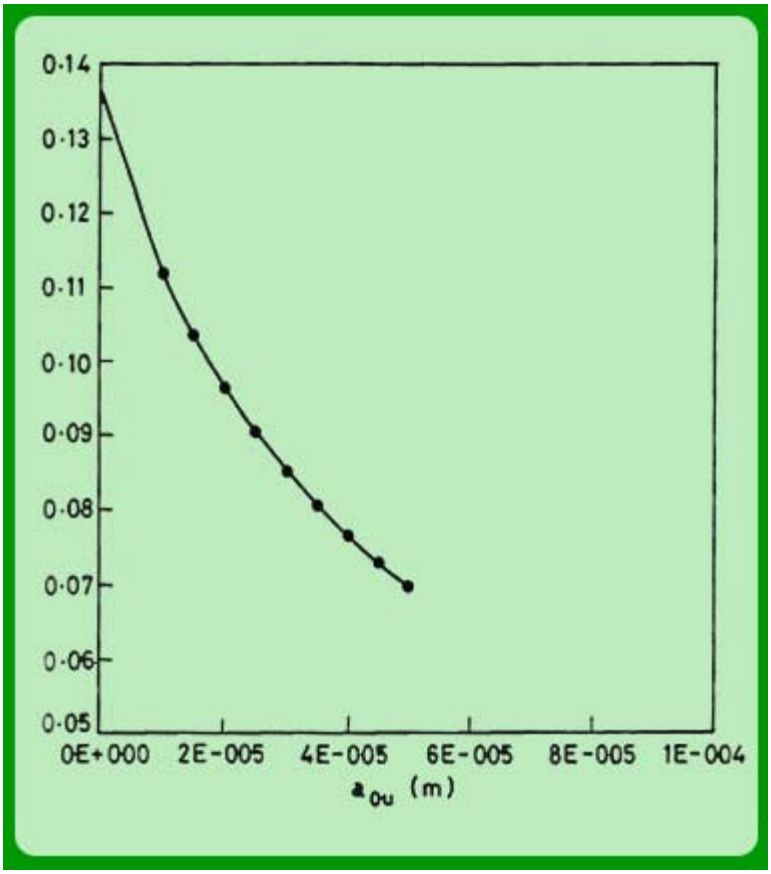

Figure 24.9 F-parameter dependence on a_{0u}

Working near the stability borders involves making a compromise on the modulation efficiency. It should be mentioned that for the typical astigmatically compensated folded cavity used in practice it is impossible to optimize the cavity configuration for both the x and y plane. The positioning of the crystal with respect to the pump beam waist also plays an important role in the mode-locking operation. The beam profile in the laser cavity for various values of normalized power have been shown in figure 24.10 and figure 24.11 for a resonator cavity with an optimized configuration for the cases of both, the OC at the long arm end mirror and the short arm end mirror. The reduction in spot size at the output coupler end due to Kerr lensing effect of the crystal is evident in these figures (24.10 and 24.11). By placing a hard aperture of suitable dimension at the end mirror, the low power cw mode can be cut off and only the high power mode-locked beam is allowed to oscillate. The beam profiles in the crystal for the various values of normalized power are shown in 24.10 and figure 24.11.

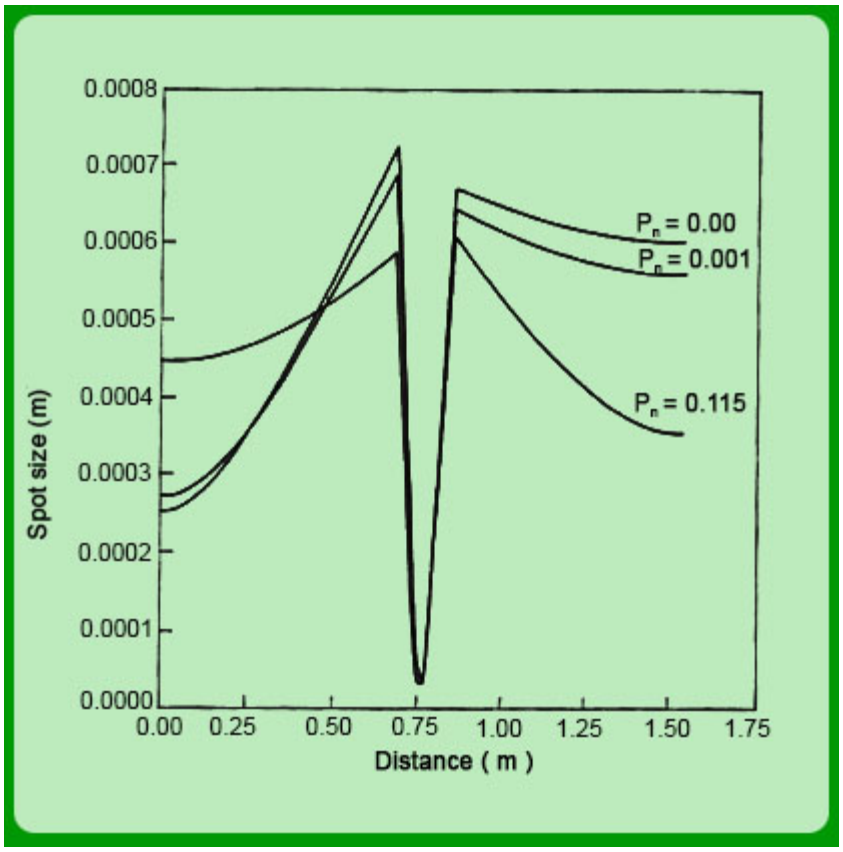

Figure 24.10 Power dependence of intracavity beam profile for OC in longer term

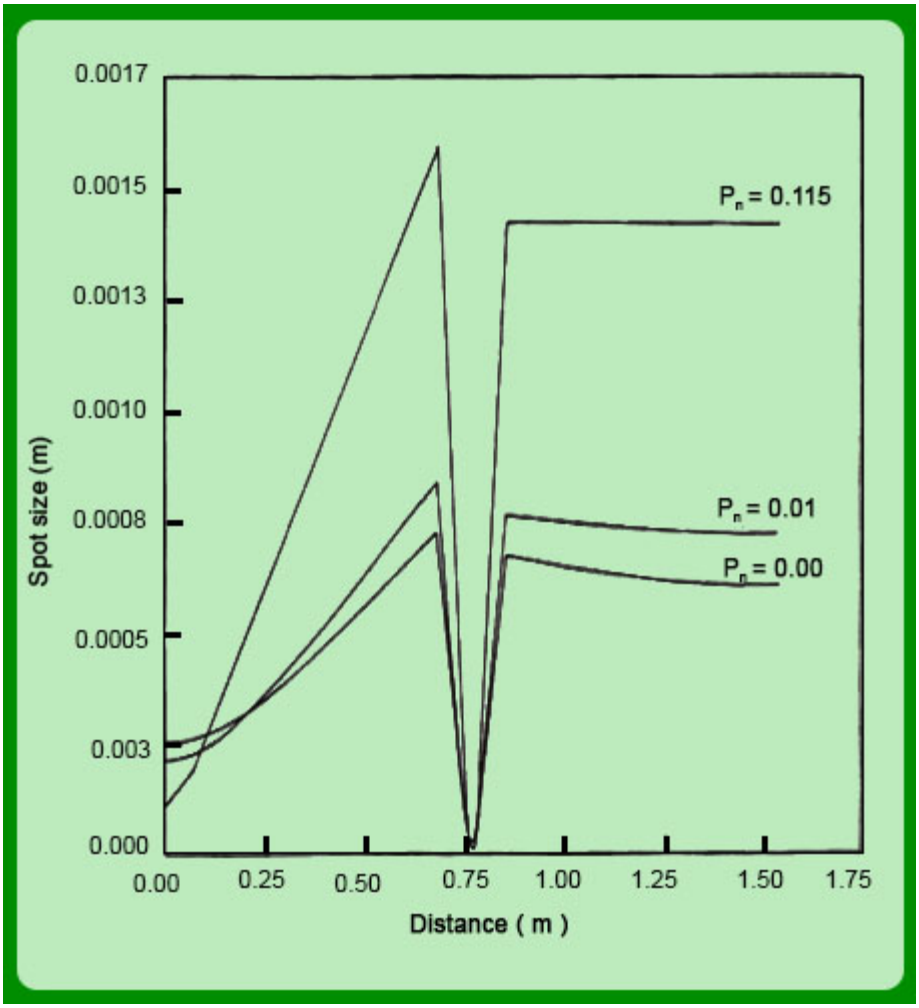

Figure 24.11 Power dependence of intracavity beam profile for OC in shorter term

The self mode locking is highly dependent on the overlap of the pump beam with the resonator mode in the crystal. The optimization of this overlap and hence the gain can be achieved by adjusting the position of pump beam focusing lens. The degree of pump beam overlap with the mode is decided by the overlap integral given by

$$\eta = \frac{\left|\int_0^l \omega_L^2(z)\,\omega_P^2(z)\,dz\right|^2}{\left|\int_0^l \omega_L^2(z)\,dz\right|^2 \left|\int_0^l \omega_P^2(z)\,dz\right|^2} \qquad (24.36)$$

where ω_L is the spot size of laser resonator mode ω_p is the spot size of the pump beam. The variation of η with the positioning of the pump beam lens is shown in the figure 24.12.

The overlap integral has been maximized by positioning the pump lens at the optimum position giving the highest overlap.

In place of a hard aperture we could have made use of the positioning of the crystal with respect to the pump beam to introduce a radially varying gain profile in the crystal which itself acts like a soft aperture. The cw mode of the laser has a broader spot size in the crystal than the high power locked-mode. The pump beam can so be adjusted that the region of the crystal being pumped discourages gain at the periphery of the crystal, thus effectively cutting out the cw mode which has a broader waist.

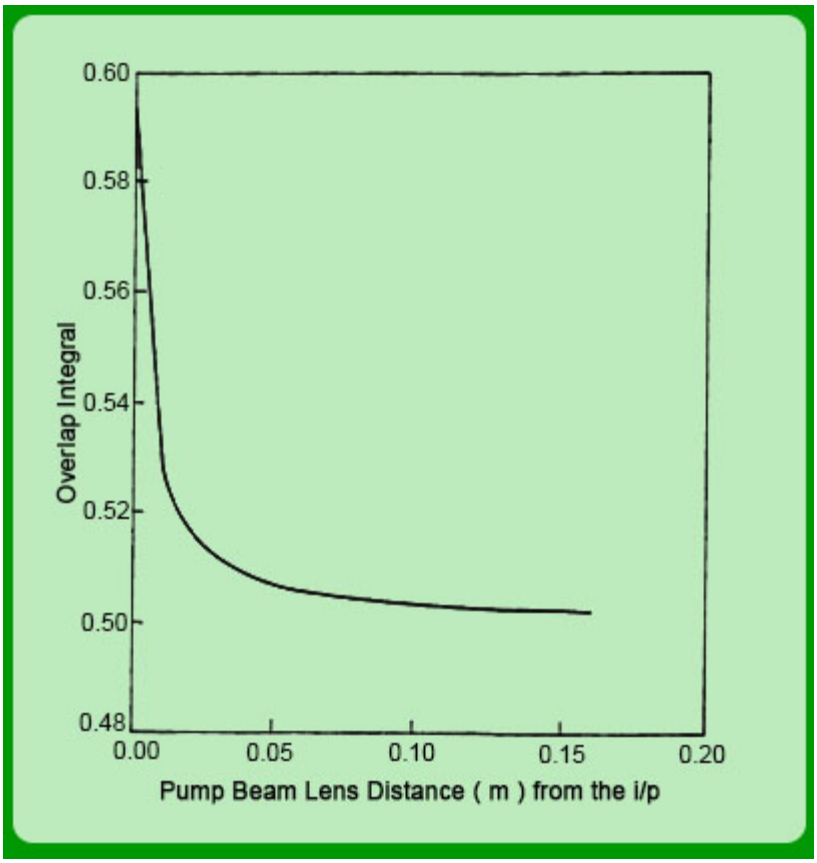

Figure 24.12 Overlap integral value as a function of pump beam lens from input end curved mirror

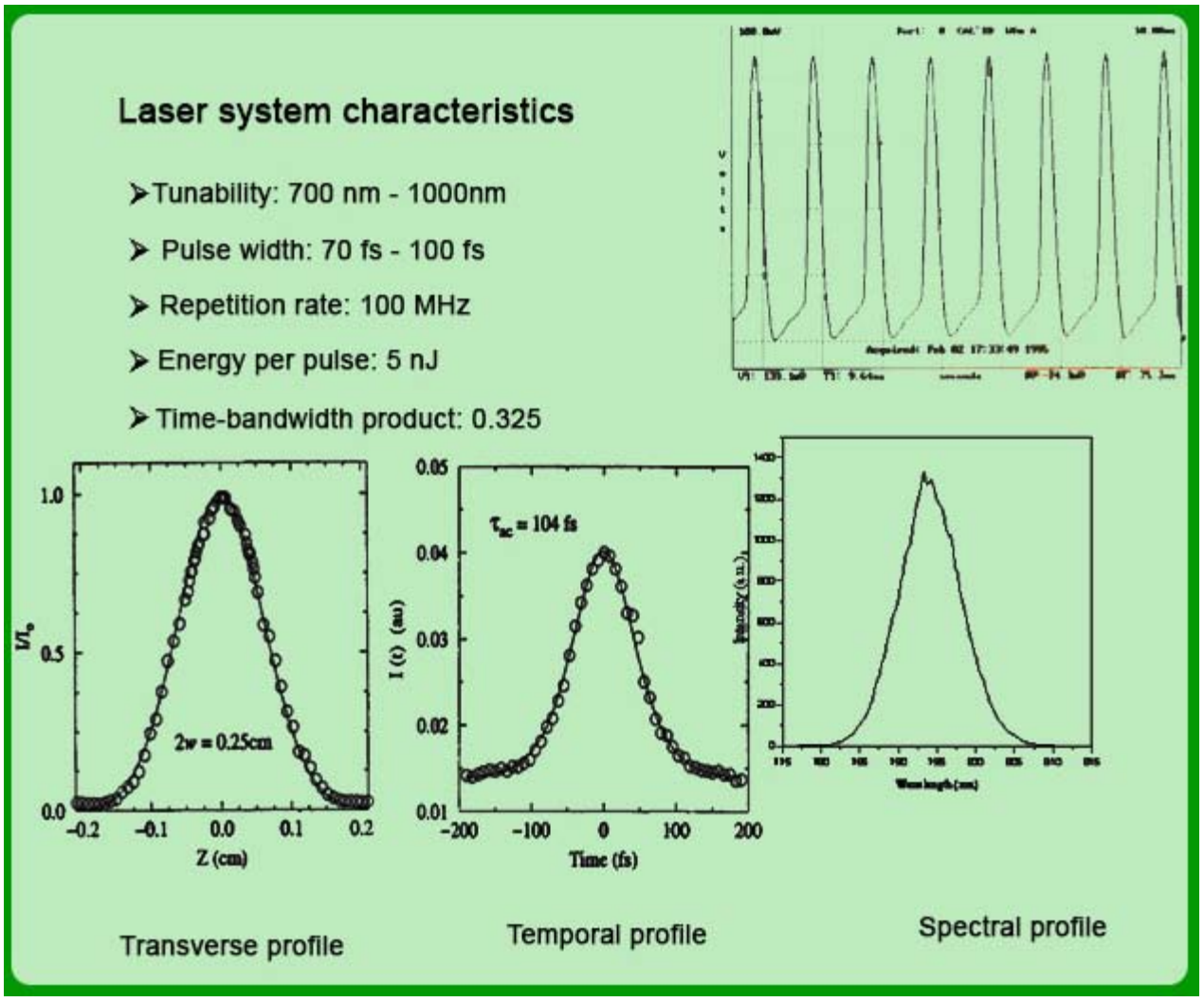

Figure 24.13

Ti:Sapphire laser cavity configured according to the dictates of the above formalism resulted in stable self modelocking of our laser. The laser delivers transform limited ~80 fs (typical) pulses at repetition rate of 100 MHz. The average output power of this laser is 600 mW at about 800 nm when pumped with 6 watts power (all line) of cw argon-ion laser. The laser performance characteristics are summarized in figure 24.13.

References:

1. V. Magni, G. Cerullo and S. D. Silvestri, Opt. Commun. **96**,348(1993).

Recap

In this lecture we have looked at the

1. Two-photon absorption process – a qualitative picture.
2. Two-photon transition rate.
3. And its application to Doppler free spectroscopy.